Journal of Cerebral Blood Flow & Metabolism (2015) 35, 2032–2042

www.jcbfm.com

ORIGINAL ARTICLE

The cumulative influence of hyperoxia and hypercapnia on blood oxygenation and R_2^*

Carlos C Faraco[1], Megan K Strother[1], Jeroen CW Siero[2], Daniel F Arteaga[1], Allison O Scott[1], Lori C Jordan[3,4] and Manus J Donahue[1,4,5]

Cerebrovascular reactivity (CVR)-weighted blood-oxygenation-level-dependent magnetic resonance imaging (BOLD-MRI) experiments are frequently used in conjunction with hyperoxia. Owing to complex interactions between hyperoxia and hypercapnia, quantitative effects of these gas mixtures on BOLD responses, blood and tissue R_2^*, and blood oxygenation are incompletely understood. Here we performed BOLD imaging (3 T; *TE/TR* = 35/2,000 ms; spatial resolution = $3 \times 3 \times 3.5$ mm^3) in healthy volunteers ($n = 12$; age = 29 ± 4.1 years) breathing (i) room air (*RA*), (ii) normocapnic–hyperoxia (95% O_2/5% N_2, *HO*), (iii) hypercapnic–normoxia (5% CO_2/21% O_2/74% N_2, *HC-NO*), and (iv) hypercapnic–hyperoxia (5% CO_2/95% O_2, *HC-HO*). For *HC-HO*, experiments were performed with separate *RA* and *HO* baselines to control for changes in O_2. T_2-relaxation-under-spin-tagging MRI was used to calculate basal venous oxygenation. Signal changes were quantified and established hemodynamic models were applied to quantify vasoactive blood oxygenation, blood–water R_2^*, and tissue–water R_2^*. In the cortex, fractional BOLD changes (stimulus/baseline) were *HO/RA* = 0.011 ± 0.007; *HC-NO/RA* = 0.014 ± 0.004; *HC-HO/HO* = 0.020 ± 0.008; and *HC-HO/RA* = 0.035 ± 0.010; for the measured basal venous oxygenation level of 0.632, this led to venous blood oxygenation levels of 0.660 (*HO*), 0.665 (*HC-NO*), and 0.712 (*HC-HO*). Interleaving a *HC-HO* stimulus with *HO* baseline provided a smaller but significantly elevated BOLD response compared with a *HC-NO* stimulus. Results provide an outline for how blood oxygenation differs for several gas stimuli and provides quantitative information on how hypercapnic BOLD CVR and R_2^* are altered during hyperoxia.

Journal of Cerebral Blood Flow & Metabolism (2015) **35,** 2032–2042; doi:10.1038/jcbfm.2015.168; published online 15 July 2015

Keywords: BOLD; cerebrovascular reactivity; hypercapnia; hyperoxia; R_2*

INTRODUCTION

Assessment of hemodynamic impairment is critical when informing management decisions in patients with cerebrovascular disease. Clinically, evolution of cerebrovascular compromise is most commonly assessed with either computed tomographic angiography or catheter angiography, both of which are sensitive to intra-luminal changes but are not directly sensitive to tissue-level hemodynamics. As these methods require radiation exposure and exogenous contrast agents, they are also sub-optimal for longitudinal monitoring of reperfusion or hemodynamic decline.

A possible alternative, or complement, to conventional imaging is hypercapnia-induced cerebrovascular reactivity (CVR)-based mapping using magnetic resonance imaging (MRI) modalities such as blood-oxygenation-level-dependent (BOLD) and/or arterial spin labeing (ASL) MRI.[1–4] In such methods, a vasoactive stimulus is administered pharmacologically[5,6] or through a hypercapnic respiratory challenge[7–9] of mildly elevated CO_2 (e.g., 4% to 6% CO_2 in balance air), which relaxes arteriolar smooth muscle leading to an increase in cerebral blood flow and volume (*CBF* and *CBV*, respectively) in healthy tissue, yet a smaller,[10,11] negligible,[12,13] or even negative[12,14] change in *CBF* and *CBV* in parenchyma operating at or near reserve capacity. Such hypercapnic CVR measurements have been shown to correlate with cortical thickness,[15] symptomatology,[10] catheter angiography-measured arterial circulation times,[16] and vasculopathy extent.[10,17]

CVR mapping using non-invasive hypercapnic stimuli is an appealing alternative to other approaches that require pharmacological or exogenous contrast agents; however, obvious concerns related to eliciting hypercapnia in patients with low blood oxygenation and/or ischemic tissue preclude widespread application. To reduce these concerns, it is also possible to administer a hypercapnic–hyperoxic (*HC-HO*; e.g., 5% CO_2/95% O_2) gas for short durations, with the expectation that the *HO* component of the gas mixture may increase oxygen delivery to tissue even in the presence of *HC*.[18,19] In a recent trial of 92 patients with symptomatic cerebrovascular disease, no immediate stroke-related complications were reported in response to *HC-HO* administration and the frequency of longer-term (6 to 18 months) neurologic events was within the range for expected events in this patient population.[10]

Administration of a *HC-HO* gas mixture for BOLD-weighted assessment of CVR introduces several experimental confounds because of the *HO* component,[10,20–23] including (i) higher venous HbO_2 and elevated partial pressure of venous oxygen (PvO_2) from increased O_2 dissolved in plasma, (ii) changes in vascular and tissue susceptibility due to increased HbO_2, and (iii) increased blood water R_1 due to increased O_2 dissolved in plasma. Although the effect of (iii) is likely small in minimally T_1-weighted BOLD acquisitions, contributions from (i) and (ii) may be much larger, and appropriate methods for compensating for these confounds

[1]Department of Radiology and Radiological Sciences, Vanderbilt University Medical Center, Nashville, Tennessee, USA; [2]Department of Radiology, University Medical Center Utrecht, Utrecht, The Netherlands; [3]Department of Pediatric Neurology, Vanderbilt Children's Hospital, Nashville, Tennessee, USA; [4]Department of Neurology, Vanderbilt University Medical Center, Nashville, Tennessee, USA and [5]Department of Psychiatry, Vanderbilt University Medical Center, Nashville, Tennessee, USA. Correspondence: Dr MJ Donahue, Vanderbilt University Institute of Imaging Science, Medical Center North, AAA-3115, 1161 21st Avenue South, Nashville, Tennessee 37232, USA.
E-mail: mj.donahue@vanderbilt.edu
Funding was provided by the American Heart Association 14CSA20380466 and National Institutes of Health (NIH/NINDS) 5R01NS078828.
Received 26 January 2015; revised 9 June 2015; accepted 11 June 2015; published online 15 July 2015

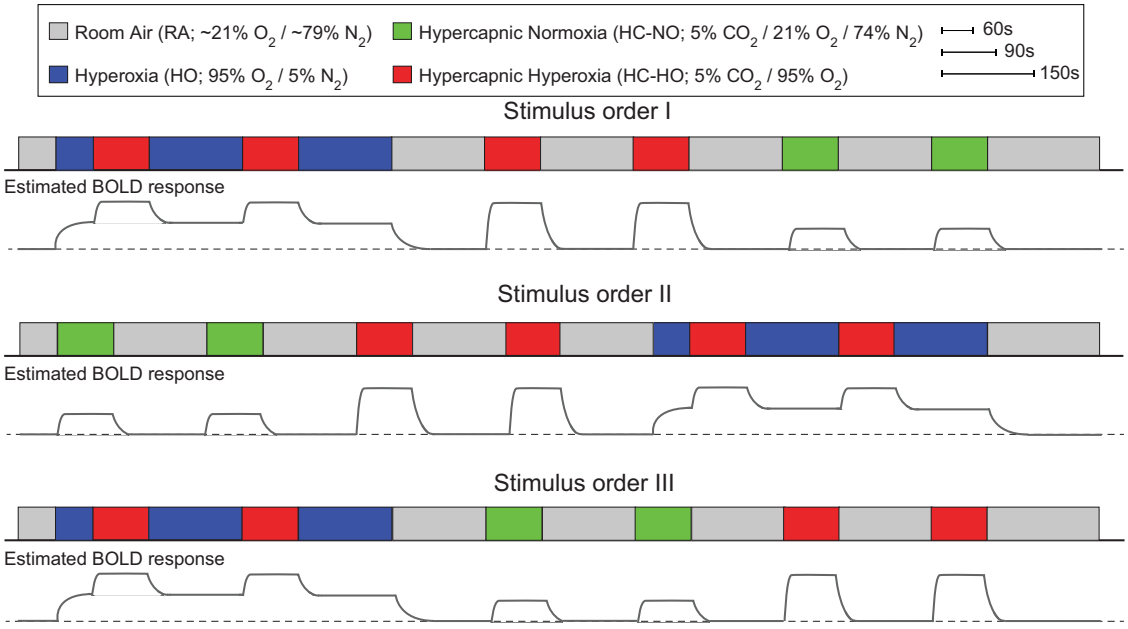

Figure 1. The respiratory stimulus consisted of alternating 90-second (stimulus) and 150-second (baseline) gas pairings, each repeated twice. The total paradigm lasted approximately 29 minutes and was randomized in three different orderings (I to III) across the 12 healthy volunteers. BOLD, blood-oxygenation-level-dependent.

have not been established. As such, the use of *HC-HO* for quantitative BOLD-weighted CVR assessment remains poorly developed.

The aim of the current study was to address these limitations by assessing CVR measurements obtained using straightforward *HC-NO* gas challenges and those obtained using a *HC-HO* stimulus interleaved with a *HO* baseline period. The *HO* baseline period was introduced to control for dynamic changes in O_2 that would otherwise occur between room air (*RA*) breathing and *HC-HO* stimuli, with the overall hypothesis that *HC-HO* stimuli interleaved with a *HO* baseline would provide a comparable CVR measurement to a *HC-NO* stimulus interleaved with a *RA* baseline. To evaluate the quantitative changes occurring in blood oxygenation for the different gas mixtures, established BOLD contrast models of blood and tissue R_2^* were applied together with multivariate fitting. The results of this study are intended to better inform clinical applications of CVR assessment in patients in whom *HC-NO* stimuli may be contraindicated.

MATERIALS AND METHODS

Volunteer Demographics

Healthy volunteers ($n = 12$; 3 F/9 M; age = 29 ± 4.1 years) provided informed, written consent in accordance with the ethical standards of the Vanderbilt University Institutional Review Board, the Vanderbilt University Human Research Protection Program, as well as with the Helsinki Declaration of 1975 (and as revised in 1983). All components of this study were in compliance with the Health Insurance Portability and Accountability Act. All study components were reviewed and approved by the local Institutional Review Board (IRB Study 111116).

MRI Experiment

MRI measurements were performed at 3.0 T (Philips Healthcare, Best, The Netherlands). Participants were fitted with a nasal cannula (Salter Labs, Arvin, CA, USA, no. 4000) for end-tidal CO_2 ($EtCO_2$) monitoring and a custom non-rebreathing oxygen mask (Salter Labs, no. 8005) for gas stimulus administration. Participants wore close-fitting masks that covered the nose and mouth and elastic straps were used to reduce leakage. Gases were delivered from compressed cylinders outside the scan room and administered at 12 L/min. This flow rate was optimized in preliminary studies and was found to provide sufficient gas delivery in the presence of potential small leaks in the mask, while also maintaining comfort. The repeatability of this setup has been reported in previous work.[24] Physiologic monitoring was performed using an Invivo Research (Gainesville, FL, USA) (3150 MRI) monitor and a remote monitor (Millenia Vital System, Gainsville, FL, USA, 3115 MVS). Monitored parameters included $EtCO_2$ (mm Hg), arterial oxygenation (Y_a), and heart rate (*HR*; b.p.m.); participants were fitted with a pulse-oximeter to measure Y_a and *HR*.

The stimulus paradigm consisted of a 29-minute run during which subjects were presented with periods of hypercapnic stimuli interleaved with a baseline gas (*RA* or *HO*) which included:

(i) Hypercapnic–normoxia (*HC-NO*; 5% CO_2/21% O_2/74% N_2) interleaved with room air (*RA*; ~21% O_2/~79% N_2),
(ii) Hypercapnic–hyperoxia (*HC-HO*; 5% CO_2/95% O_2) interleaved with RA, and
(iii) Hypercapnic–hyperoxia (*HC-HO*) interleaved with hyperoxia (*HO*; 95% O_2/5% N_2).

Each baseline period lasted 150 seconds while each stimulus period lasted 90 seconds. Each respiratory challenge (e.g., stimulus and baseline block) was repeated twice in each volunteer, and the pairing order was randomized across all subjects. Single-shot gradient-echo Cartesian EPI BOLD acquisitions were acquired using body coil transmit and an eight-channel SENSE head coil (Nova Medical, Waltham, MA, USA) for reception with $TE/TR = 35/2{,}000$ ms, spatial resolution = $3 \times 3 \times 3.5$ mm^3, SENSE-factor = 2. T_1-weighted high spatial resolution 3D anatomic turbo gradient echo images (MPRAGE) were acquired for all subjects ($TE/TR = 4.6/8.9$ ms; spatial resolution = $1 \times 1 \times 1$ mm^3). Figure 1 illustrates the three orders of the stimulus paradigms as well as a schematic of the relative magnitude of the hypothesized BOLD responses given the variations in blood oxygenation.

Finally, to quantify the baseline venous oxygenation level, which is required for quantitative determination of blood oxygenation changes with different gas stimuli, we applied the T_2-relaxation-under-spin-tagging (TRUST)[25] method in all subjects during *RA* breathing. In this approach, venous blood water signal in the superior sagittal sinus is isolated using principles of venous spin labeling, and a T_2-preparation module is used to allow for variable T_2 weighting and venous T_2 to be quantified. The venous T_2 is then related to venous blood oxygenation level using calibration models that describe the dependence between T_2, oxygenation level and hematocrit (*Hct*).[26] Specifically, following venous blood water labeling

using a PICORE labeling module, a postlabeling delay time of 1,022 ms was used, during which the labeled venous blood water flows into the imaging region. During this period, a T_2-preparation module was applied with varying duration (effective TE, *eTE*). The T_2-preparation module consisted of a non-selective 90° pulse followed by a string of refocusing pulses with constant inter-pulse spacing ($\tau = 10$ ms) and concludes with a $-90°$ pulse. Here the T_2 module was performed for $eTE = 0$, 40, 80, and 160 ms (four averages per *eTE*; $TR = 1{,}978$ ms). Following the T_2-preparation, a single-shot gradient echo EPI readout was applied, and the sequence concluded with a postsaturation excitation pulse and dephasing gradient for spin reset.

Analysis

All TRUST processing used in-house MATLAB (Mathworks, Natick, MA USA) scripts. Data were motion-corrected and pair-wise subtracted to obtain a difference magnetization image for each of the four eTEs, and four voxels within the sagittal sinus were analyzed per subject. Owing to distal venous labeling and identical magnetization transfer effects in control and label conditions, the tissue signals in control and label conditions are identical and can be neglected when analyzing the difference signal. A previously published quantification procedure was applied[26] in which male *Hct* was assumed to be 0.42 and female *Hct* 0.40 in the superior sagittal sinus. This analysis pipeline is identical to that which has been outlined in the literature.[27]

BOLD-weighted data were slice-time corrected and affine motion corrected using routines available in the FMRIB Software Library (FSL).[28] For each participant, T_1-weighted images were segmented into gray matter (GM), white matter, and cerebrospinal fluid using the FMRIB Automated Segmentation Tool (FAST).[28]

In-house Matlab (Mathworks) routines were used for baseline drift correction and signal extraction. Specifically, baseline drift correction for the entire time course was performed on a voxel-wise basis by quadratic polynomial regression, as outlined in the literature.[29,30] This procedure was pursued to maintain signal change differences between different stimulus types that may be altered when using temporal filtering for drift correction.

Fractional signal change maps ($\Delta S/S$; signal difference between baseline and stimulus over baseline signal) were calculated for each pair of stimulus blocks (two maps per condition), as well as an averaged signal change map, by comparing values from the last 15 *TRs* of the respiratory stimulus to the last 30 *TRs* of the proceeding baseline condition. These periods were conservatively chosen to ensure that the signal had reached a plateau in stimulus epochs or had normalized in the baseline states; both of these conditions were further ensured by verifying that recorded $EtCO_2$ values were not changing significantly.

Regions of interest for analysis of each baseline/stimulus pairing were calculated in two ways. First, for each participant, *Z*-statistic maps for each baseline/stimulus pairing were calculated from the preprocessed (slice-time, motion, and baseline drift corrected) data using FSL's FEAT;[28] FILM prewhitening was used for statistical processing. Resulting *Z*-statistics maps were thresholded at *Z*-value $\geqslant 2$ ($\geqslant$2 standard deviations above mean baseline signal) and binarized. The three resulting masks were then multiplied into a single mask which represented voxels that were activated in all three stimulus conditions. This *Z*-statistic mask was then multiplied by a once-eroded brain mask calculated using FSL's Brain Extraction Tool (BET)[28] to ensure that only brain voxels were considered. The averaged *Z*-statistic map was then used to extract signal change values across all three conditions as well as stimulus time courses for those voxels. Although the above approach ensures that only voxels responding to all vasoactive stimuli are considered, it also biases the region of interest for voxels with larger venous blood volume where BOLD effects are highest. Therefore, we additionally extracted BOLD signal changes using GM masks from each subject, which were obtained by segmenting each subject's T_1 image using FSL's FAST, warping the GM masks to BOLD GRE image space using an affine transformation and nearest neighbor interpolation in the FMRIB Linear Image Registration Tool (FLIRT),[28] thresholding the resulting GM masks at a value of 0.5, and binarizing the masks. Additionally, as some regions in the GM mask have low signal-to-noise ratio in BOLD GRE space because of EPI distortion, GM masks were multiplied by twice eroded brain masks calculated from the BOLD data to ensure that regions outside the brain were not considered.

Finally, signal change maps were co-registered to a standard atlas (Montreal Neurological Institute; spatial resolution = 4 mm isotropic)[31] using FLIRT to generate group-averaged signal change maps for visualization; 4 mm^3 space was chosen to approximately match the original acquisition's spatial resolution.

Statistical Considerations

The primary experimental objective of this study was to assess the relationship between the study co-variates (e.g., gas stimulus type) and the BOLD signal change. Secondary objectives were to ensure repeatability of the CVR responses across volunteers and the different stimulus orderings, to directly compare the BOLD responses between the different gas stimulus pairings of interest, and to model the changes in blood oxygenation and R_2^* for different gas combination (see Blood oxygenation and R_2^* quantification). To test the primary objective, a two-tailed Student's *t*-test was used to evaluate differences in GM signal changes and physiologic parameters between gas conditions with Bonferroni-corrected criteria for significance at $P < 0.017$ (signal change comparisons for the three gas pairings; total of three comparisons) and $P < 0.008$ ($EtCO_2$ comparisons for all gases; total of six comparisons), respectively. To test the CVR repeatability and CVR relationships for the gas stimuli, Pearson's correlation coefficients and linear models were applied to BOLD responses extracted using the *Z*-statistic and GM masks. Slopes and intercepts of comparisons were recorded.

Although changes in $EtCO_2$ ($\Delta EtCO_2$) were measured in all subjects, our focus was primarily to interpret quantitative BOLD signal changes in terms of R_2^* and blood oxygenation level. To enable application of physiologic models, BOLD responses were not normalized by $\Delta EtCO_2$. Instead, we verified that for each subject, hypercapnic signal change data occurred during an $EtCO_2$ increase in an expected range (4 to 8 mm Hg) and that mean $EtCO_2$ increases did not differ significantly on average between hypercapnic gas stimuli for each subject. As such, results in this study are presented in terms of signal changes rather than signal changes normalized by $EtCO_2$ change. $\Delta EtCO_2$ is reported for all gas stimuli for completeness.

Blood Oxygenation and R_2^* Quantification

The purpose of this component of the study was to combine the data from different gas stimuli with previously published models of BOLD contrast and perform multivariate fitting to quantify the changes in venous blood oxygenation (Y_v). This procedure used our experimental findings of BOLD responses and baseline oxygenation-level status and applied previously published integrative, quantitative physiologic models of BOLD contrast. To achieve this, (i) BOLD signal changes were written in terms of blood oxygenation for each of the three different gas stimuli, (ii) R_2^* for blood[32] and tissue[33] were calculated using previously published models, and (iii) the residual sum of squares (*RSS*) between the experimentally measured signal changes and the model was minimized by simultaneously solving for blood oxygenation status under the conditions of *HO*, *HC-NO*, and *HC-HO* using a generalized reduced gradient nonlinear algorithm.

More specifically, the brain parenchyma can be divided into extravascular (e.g., tissue water) and microvascular (e.g., capillary+arteriole +venule water) compartments. Under conditions of breathing *RA*, in cortical GM at typical fMRI spatial resolutions, prior *CBF* and *CBV* measurements have shown that extravascular tissue occupies approximately 0.945 of a parenchymal voxel, while the remaining 0.055 can be approximated as 0.30 arteriolar blood and 0.70 venular blood.[34,35] For non-hypoxic healthy adults, changes in Hb oxygen saturation with gas stimuli primarily occur in venous blood, which influence both the venous R_2^* and tissue R_2^*. The effect of the gas stimuli on the total BOLD-weighted MR signal in the voxel (S_{voxel}) in terms of the arteriolar ($S_{blood,a}$), venular ($S_{blood,v}$), and tissue (S_{tissue}) signals can be written:

$$S_{voxel,j} = S_{blood,a,j} + S_{blood,v,j} + S_{tissue,j} \quad (1)$$

for j = (base)line or (act)ivation (applicable here and for all future equations). The separate blood and tissue signals in Equation 1 can be expanded in terms of water density (*C*; mL/mL), blood compartment fraction (*f*b), *CBV* (mL/mL), *TR* (s), R_1 (1/s), *TE* (s), and R_2^* (1/s):

$$S_{blood,i,j} = C_b \cdot fb_{i,j} \cdot CBV_j \cdot \left(1 - e^{-TR \cdot R_{1,i,j}}\right) \cdot e^{-TE \cdot R^*_{2,i,j}} \quad (2)$$

for i = (a)rterial or (v)enous blood, and

$$S_{tissue,j} = C_t \cdot (1 - CBV_j) \cdot \left(1 - e^{-TR \cdot R_{1,t}}\right) \cdot e^{-TE \cdot R^*_{2,t,j}} \quad (3)$$

Here baseline and activation (subscript j) refers to the gas condition being used and could be *RA*, *HO*, *HC-NO*, or *HC-HO*. It should also be noted that during activation the *CBV* change is primarily arterial; therefore, 2 may have $fb_{v,base} = fb_{v,act}$, but $fb_{a,base} < fb_{a,act}$. Both conditions were evaluated here. All parameters used, along with literature references, are included in Table 2. Below we provide a brief explanation for the choice of these parameters. $C_b = 0.87$ mL water/mL blood is the blood water

Table 1. Mean physiology measurements and ΔS/S for the gas pairings

Gas pairing	$\Delta EtCO_2$ *(mm Hg)*	ΔY_a	ΔHR *(b.p.m.)*	ΔS/S *(activation mask)*	ΔS/S *(gray matter mask)*
HO/RA	−1.17 ± 2.19	0.0097 ± 0.0073	−0.90 ± 5.30	0.027 ± 0.014	0.011 ± 0.007
HC-NO/RA	5.59 ± 2.00	−0.0004 ± 0.0033	1.10 ± 3.31	0.034 ± 0.007	0.014 ± 0.004
HC-HO/HO	5.68 ± 1.87	0.0006 ± 0.0009	0.15 ± 1.41	0.044 ± 0.014	0.020 ± 0.008
HC-HO/RA	5.75 ± 2.11	0.0076 ± 0.0061	−0.18 ± 1.69	0.084 ± 0.017	0.035 ±0.010

HC-HO, hypercapnic hyperoxia; *HC-NO*, hypercapnic normoxia; *HO*, hyperoxia; *RA*, room air. Mean ± standard deviation of the change in end-tidal CO_2 ($\Delta EtCO_2$), arterial oxygen saturation fraction (ΔY_a), and heart rate (ΔHR) for the three gas pairings of interest and *HO/RA*. To the right, the blood-oxygenation-level-dependent signal changes normalized by baseline signal ($\Delta S/S$) are shown separately when calculated using the activation mask or GM mask.

density, $C_t = 0.89$ mL water/mL tissue is the tissue water density, $CBV_{base} = 0.055$ mL/mL, $fb_{a,base} = 0.3$ and $fb_{v,base} = 0.7$ are the baseline fractional contributions to total *CBV* of the arterial and venous compartments, respectively.[35] The total *CBV* has been calculated from recent *CBF* data that accounted for bolus arrival time and used the same pCASL and gas delivery setup as applied here.[24] In this study, $CBF_{RA} = 43 \pm 6$ mL/100 g/min and $CBF_{HC\text{-}NO} = 48 \pm 8$ mL/100 g/min, which upon application of the Grubb relationship[36] yields $CBV_{HC\text{-}NO} = 0.0574$ mL/mL. Here, owing to a lack of conclusive data showing changes in *CBV* with hyperoxia,[23,37] we assumed $CBV_{RA} = CBV_{HO}$ and $CBV_{HC\text{-}NO} = CBV_{HC\text{-}HO}$; therefore, $fb_{a,act} = 0.329$ and $fb_{v,act} = 0.671$. This assumption is also addressed by considering a condition where *CBV* reduces by 0.001 mL/mL with hyperoxia. For R_1 of arterial and venous blood water, all normoxic conditions used $R_{1,a} = 0.572$/s and $R_{1,v} = 0.587$/s, which was based on *in situ* data from bovine blood, and assuming an intermediate voxel $Hct = 0.37$. Note that a reduced *Hct* was used here, relative to what was used in the TRUST analysis, as this *Hct* pertains to the mean *Hct* within a voxel whereas the TRUST *Hct* refers to the *Hct* in the superior sagittal sinus. During hyperoxia, it is well known that dissolved oxygen in plasma will increase the R_1 of arterial blood water; this change has recently been estimated from *in vivo* ASL data obtained during different gas stimuli, and a value of $R_{1,a,HH} = 0.630$/s was used here. The venous R_1 is not expected to change substantially with hyperoxia, and therefore $R_{1,v,HO} = R_{1,v,HC\text{-}HO} = R_{1,v,RA}$. A hypothetical condition where hyperoxic venous blood water R_1 increases by the same amount as the hyperoxic arterial blood water R_1 was considered as a supplementary analysis to understand the impact of this assumption. Finally, $R_{1,t} = 0.83$/s.[38]

The remaining unknowns are the $R^*_{2,t}$ and blood R^*_2 parameters, which can both be written in terms of the blood oxygenation using previously reported integrative models[33] that are based on primarily *in vivo* BOLD signal changes and *in situ* measurements of blood relaxation times at multiple field strengths.[32]

First, $R^*_{2,t}$ depends on blood oxygenation and vessel size as has been elegantly summarized;[33] initially, $R^*_{2,t}$ can be calculated for 100% arterial and venous oxygenation, which indicates the condition at which there would be no susceptibility differences between the extravascular and intravascular compartments due to oxygenation differences,[33]

$$R^*_{2,t,j} = R^*_{2,0,t} + R^*_{2,Hb,t,j} \tag{4}$$

where $R^*_{2,0,t}$ is the intrinsic effective transverse relaxation rate for tissue in the absence of contributions from Hb, and $R^*_{2,Hb,t}$ specifically describes the contribution to $R^*_{2,t}$ from Hb. $R^*_{2,0,t}$ has been reported to be

$$R^*_{2,0,t} = (3.74/T \cdot s) \cdot B_0 + 9.77/s \tag{5}$$

or $R^*_{2,0,t} = 20.99/s$ at 3 T. Note that this value does not change for different gas stimuli. As reductions in intravascular oxygenation (Y) cause a Larmor frequency shift, Δv_s, which increases susceptibility at the vessel surface and increases $R^*_{2,Hb,t}$, Δv_s will evolve according to,[33]

$$\Delta v_{s,j} = \frac{\Delta\chi_0}{4 \cdot \pi} \cdot Hct \cdot \left(\left|Y_{off} - Y_j\right|\right) \cdot \gamma \cdot B_0 \tag{6}$$

where $\Delta\chi_0 = 4 \times \pi \times 0.264$ p.p.m. is the susceptibility difference between fully oxygenated and deoxygenated blood, $Hct = 0.37$ is mean GM voxel hematocrit,[34,39] $Y_{off} = 0.95$ is the oxygenation equilibrium state (different from the measured arterial oxygenation level),[33,40] Y is the blood oxygenation level, and $\gamma = 2\pi \times 42.6$ MHz/T is the gyromagnetic ratio. Δv_s was only calculated for Y_v as Y_a is close to 100% in healthy subjects and any changes in susceptibility are negligible. For gradient-echo scans it is possible to express $R^*_{2,Hb,t}$ in different vessel compartments using a polynomial function that depends explicitly on Δv_s[33] and coefficients that are unique for vessels of different sizes. Here, following literature assumptions, we estimate that the venous blood volume (CBV_v; the fraction of blood that undergoes changes in blood oxygenation with the respiratory challenges) in a GM voxel is composed of approximately 50% venous capillaries and 50% venules (diameter = 16 to 200 μm). We did not include large vessel (> 200 μm) contributions as our simulation was based on masks derived from GM voxels within an eroded brain mask (see Analysis), which is expected to partial volume minimally with large draining veins. The $R^*_{2,Hb,t}$ can then be written,

$$R^*_{2,Hb,t,j} = \left[\left(b_1 \cdot \Delta v^4_{s,j} + c_1 \cdot \Delta v^3_{s,j} + d_1 \cdot \Delta v^2_{s,j} + e_1 \cdot \Delta v^1_{s,j} + f_1\right) + \left(b_2 \cdot \Delta v^4_{s,j} + c_2 \cdot \Delta v^3_{s,j} + d_2 \cdot \Delta v^2_{s,j} + e_2 \cdot \Delta v^1_{s,j} + f_2\right)\right] \cdot (0.5 \cdot CBV_v) \tag{7}$$

Note that the fitted coefficients were calculated for percentage of *CBV* (e.g., *CBV* mL/mL × 100) and therefore CBV_v in 7 must be provided in percentage of *CBV*. Under all conditions, $CBV_v = 0.0385$ mL/mL or 3.85%. The polynomial coefficients and constant f term for venous capillaries (b–f; denoted with subscript 1) are $b_1 = 5.04e^{-9}s^3$, $c_1 = -3.05e^{-6}s^2$, $d_1 = 6.17e^{-4}s$, $e_1 = -8.02e^{-4}$, and $f_1 = -0.005$/s. The polynomial coefficients and constant f term for venules (b–f; denoted with subscript 2) are $b_2 = 0s^3$, $c_2 = 0s^2$, $d_2 = -3.56e^{-6}s$, $e_2 = 0.0453$, and $f_2 = -0.194$/s. The $R^*_{2,Hb,t}$ calculated from 7 for an equal composition of venous capillaries and venules will lead to an increase in $R^*_{2,t}$ that depends on the Y_v (which manifests within the Δv_s terms) and CBV_v.

Blood transverse relaxation rates were calculated from models developed *in situ* in bovine blood scanned over a range of *Hct* and oxygenation levels at 3 T under physiologic temperature (3.0 T; $Hct = 0.37$):[32]

$$R^*_{2,i,j} = \left(16.6 + 99.6\left(1 - Y_{i,j}\right)^2\right)^{-1} \tag{8}$$

for i = a or v.

Therefore, the above equations allow for the intravascular and extravascular R^*_2 to be written explicitly in terms of the blood oxygenation level. As such, it is possible to perform multivariate fitting to the signal changes under different conditions to quantify the blood oxygenation level and R^*_2.

We used a multivariate fitting routine to minimize the signal change error, calculated as the RSS, by solving for Y_v values for the different gas conditions. Two scenarios for minimization were used, (i) constrained fitting: $Y_{v,HC\text{-}HO}$ is an additive effect of $Y_{v,HO}$ and $Y_{v,HC\text{-}NO}$ such that:

$$Y_{v,HC-HO} = Y_{v,RA} + \left(Y_{v,HO} - Y_{v,RA}\right) + \left(Y_{v,HC-NO} - Y_{v,RA}\right) \tag{9}$$

and (ii) unconstrained fitting: $Y_{v,HC\text{-}HO}$ may contain an interaction effect between $Y_{v,HO}$ and $Y_{v,HC\text{-}NO}$ and thus was a free parameter in the fitting; $Y_{v,RA}$ was measured from the experimental TRUST data. All values used and calculated for the signal estimations are presented in Tables 1 and 2. As the activation map region of interest will bias the region for voxels with higher venous blood volume fractions and larger draining veins, we used a GM mask to calculate the signal changes for all multivariate fitting procedures.

RESULTS

Physiologic Monitoring and Signal Change Reproducibility

Table 1 summarizes the results from the physiologic monitoring during each breathing condition. Mean ± s.d. Y_v during *RA* breathing from the TRUST acquisition was 0.632 ± 0.060. Mean ± s.d. $EtCO_2$: *RA* = 43.4 ± 3.9 mm Hg; *HC-NO* = 49.0 ± 3.8 mm Hg;

Table 2. Multivariate fitting results

Stimulus	CBV_a	CBV_v	Y_a	Y_v	$R_{1,a}$ *(ms)*	$R_{1,v}$ *(ms)*	$R_{1,t}$ *(ms)*	$R^*_{2,a}$ *(ms)*	$R^*_{2,v}$ *(ms)*	$R^*_{2,t}$ *(ms)*	Δv_s	S_a	S_v	S_t	S
	Constrained fitting: $Y_{v,HC\text{-}HO} = Y_{v,RA} + (Y_{v,HO} - Y_{v,RA}) + (Y_{v,HC\text{-}NO} - Y_{v,RA})$														
RA	0.0165	0.0385	0.983	0.632	0.572	0.587	0.833	16.629	30.088	23.391	24.943	0.0055	0.0081	0.3009	0.3144
HO	0.0165	0.0385	0.989	0.659	0.630	0.587	0.833	16.612	28.191	23.112	22.837	0.0057	0.0086	0.3038	0.3182
HC-NO	0.0189	0.0385	0.979	0.665	0.572	0.587	0.833	16.644	27.779	23.049	22.356	0.0063	0.0088	0.3037	0.3187
HC-HO	0.0189	0.0385	0.987	0.710	0.630	0.587	0.833	16.617	24.976	22.600	18.825	0.0066	0.0097	0.3085	0.3248
	Unconstrained fitting:														
RA	0.0165	0.0385	0.983	0.632	0.572	0.587	0.833	16.629	30.088	23.391	24.943	0.0055	0.0081	0.3009	0.3144
HO	0.0165	0.0385	0.989	0.660	0.630	0.587	0.833	16.612	28.124	23.102	22.759	0.0058	0.0087	0.3039	0.3183
HC-NO	0.0189	0.0385	0.979	0.665	0.572	0.587	0.833	16.644	27.779	23.049	22.356	0.0063	0.0088	0.3037	0.3187
HC-HO	0.0189	0.0385	0.987	0.712	0.630	0.587	0.833	16.617	24.858	22.580	18.663	0.0066	0.0097	0.3087	0.3250

CBV, cerebral blood volume; *RA*, room air; $R_{1,a}$, R_1 of arterial blood water; $R_{1,v}$, R_1 of venous blood water; $R_{1,t}$, R_1 of extravascular tissue water; $R^*_{2,a}$, R^*_2 of arterial blood water; $R^*_{2,v}$, R^*_2 of venous blood water; $R^*_{2,t}$, R^*_2 of extravascular tissue water; Δv_s, Larmor frequency shift for the calculated Y_v; S_a, arterial signal; S_v, venous signal; S_t, extravascular signal; *S*, total intravascular and extravascular signal; Y_a, arterial oxygenation; Y_v, venous oxygenation. Multivariate fitting to determine Y_v of the various vasoactive stimuli. Constants necessary for calculation: $TR = 2{,}000$ ms; $TE = 35$ ms; $C_b = 0.87$; $C_t = 0.89$; $fb_a = 0.30$. References for parameters are as follows: CBV_a and CBV_v; van Zijl *et al.*[35] $R_{1,a}$ and $R_{1,v}$; Lu *et al.*[38] $R_{1,t}$; Lu *et al.*[42] $R_{2,a}$ and $R_{2,v}$; Zhao *et al.*[32] $R_{2,t}$ and Δv_s; Uludag *et al.*[33]

HC-HO = 48.5 ± 4.0 mm Hg; and *HO* = 42.2 ± 3.8 mm Hg. Mean ± s.d. *HRs*: *RA* = 68.4 ± 11.4 b.p.m.; *HC-NO* = 69.5 ± 10.9 b.p.m.; *HC-HO* = 67.1 ± 11.4 b.p.m.; *HO* = 67.2 ± 13.5 b.p.m. Mean ± s.d. Y_a: *RA* = 0.979 ± 0.008; *HC-NO* = 0.979 ± 0.008; *HC-HO* = 0.987 ± 0.005; *HO* = 0.989 ± 0.002. As expected, $EtCO_2$ was not found to differ significantly ($P = 0.19$) between the different hypercapnic gas stimuli but was significantly higher for both hypercapnic stimuli relative to *RA* and *HO* ($P < 0.0001$). A trend for a small $EtCO_2$ reduction was found between *RA* and *HO* ($P = 0.10$). *HR* did not differ significantly for *HC-NO* ($P = 0.29$), *HC-HO* ($P = 0.19$), or *HO* ($P = 0.44$) relative to *RA*; nor did it differ significantly between *HC-NO* ($P = 0.07$) or *HC-HO* ($P = 0.93$) relative to *HO*. *HRs* between the hypercapnic stimuli did differ significantly ($P = 0.0004$). As expected, Y_a increased mildly but significantly for *HO* ($P = 0.0006$, $P = 0.0007$) and *HC-HO* ($P = 0.001$, $P = 0.002$) relative to *RA* and *HC-NO*, respectively. No significant differences were found for Y_a between *HC-NO* and *RA* Y_a.

Figures 2A and 2B, displays the activation ($Z \geqslant 2.0$) masks along with the GM mask for a representative subject. To enable all measurements to be performed within a typical MRI scan session (i.e., approximately 1 hour), stimulus durations were 90 seconds and baseline durations 150 seconds (similar to typical hypercapnic BOLD experiments in the literature). To evaluate whether these stimulus timings and the experimental gas delivery setup provided repeatable BOLD signal changes under the three different stimulus orderings, we evaluated the consistency of the signal changes between the two blocks of each stimulus (i.e., Figure 1). A similar comparison has been reported in the literature using *CBF*.[24] Figure 2C displays representative signal change maps across each stimulus block for one subject across the three different gas pairings of interest: (1) *HC-NO/RA*, (2) *HC-HO/HO*, and (3) *HC-HO/RA*, which reflect the approximate hypothesized pattern of responses (Figure 1). As the voxel composition (e.g., venous blood volume fraction) will differ between the activation mask and GM mask, signal changes from both masks were quantified. Average fractional signal change values for each block of the gas pairings for the activation map did not differ significantly: *HC-NO/RA* = (i) 0.034 ± 0.007, (ii) 0.035 ± 0.009, $P = 0.66$; *HC-HO/HO* = (i) 0.046 ± 0.015, (ii) 0.042 ± 0.018, $P = 0.47$; and *HC-HO/RA* = (i) 0.085 ± 0.017, (ii) 0.084 ± 0.018, $P = 0.81$. For the GM mask, the relationship between gas stimuli was similar; however, the signal change magnitude was reduced: *HC-NO/RA* = (i) 0.013 ± 0.005, (ii) 0.014 ± 0.005, $P = 0.56$; *HC-HO/HO* = (i) 0.021 ± 0.009, (ii) 0.019 ± 0.009, $P = 0.37$; and *HC-HO/RA* = (i) 0.035 ± 0.010, (ii) 0.036 ± 0.011, $P = 0.73$. Stimulus repeatability was further evaluated through a Pearson's correlation which indicated that signal changes were significantly correlated (activation mask: $R^2 = 0.77$, $P < 0.001$; GM-mask: $R^2 = 0.81$, $P < 0.001$) across all subjects and all stimulus types (Figures 2D and 2E) for the two blocks of each vasoactive stimulus and baseline condition of interest.

BOLD Signal Changes in Activated and Structural Regions-of-Interest

Figures 3A–3C show representative time courses from voxels that exhibited a stimulus-evoked response ($Z \geqslant 2.0$; activation mask) for all vasodilatory gas stimuli for three representative subjects. Figures 3D and 3E show the group-averaged signal time courses for each vasodilatory stimulus for all voxels within the activation and GM masks, respectively. Although the GM mask time course exhibits lower signal changes, as expected, the time course pattern is very similar to that of the activation mask; quantitative values are summarized in Table 1.

Figures 4A–4C show the GM signal change relationships between the different gas pairings for each participant. Figure 4A demonstrates that as expected *HC-HO/RA* elicits a greater signal change than *HC-NO/RA* (slope = 1.904 and intercept = 0.0091). Although the elicited signal changes are strongly correlated ($R^2 = 0.74$, $P < 0.001$), the relationship is not one-to-one as is expected from the hyperoxia contribution, which also manifests as a non-zero intercept. This is in agreement with previously reported data demonstrating a strong correlation ($R^2 = 0.85$, $P < 0.001$) between *HC-HO/RA* and HC-NO/RA across major cortical brain lobes and cerebellum.[10] Figure 4B demonstrates that administering a *HO* baseline with a *HC-HO* challenge elicits signal changes that more closely resemble (slope = 1.404; intercept = 0.0003) those elicited during *HC-NO/RA*, while still maintaining a strong correlation to *HC-NO/RA* ($R^2 = 0.64$, $P = 0.002$). These findings support the main hypothesis of the study. Figure 4C demonstrates that, while *HC-HO/RA* elicits a greater signal change than *HC-HO/HO*, the relationship between the elicited signal changes are potentially close to being linear (slope = 0.9965) with a strong correlation of $R^2 = 0.62$, $P = 0.002$. However, the intercept is strongly positive (intercept = 0.0157), which provides support for the hyperoxic component of the stimulus affecting the magnitude of the response but not the linearity of the relationship between the gas stimuli over the measured range.

Figure 5A shows the group-averaged fractional signal change maps for the three different stimulus pairings, along with the

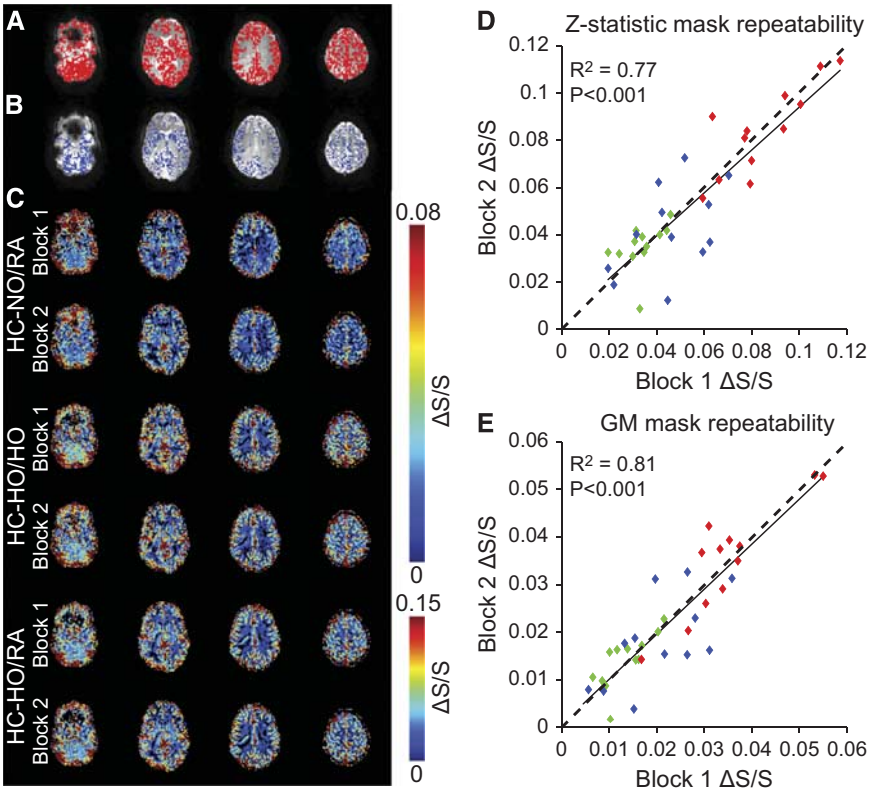

Figure 2. Regions of interest and repeatability. (**A**) *Z*-statistic mask and (**B**) gray matter mask overlaid on blood oxygenation-level-dependent gradient echo images for a representative subject. (**C**) Signal changes for each block of the respiratory stimulus. Repeatability across blocks when signal changes are calculated from the (**D**) *Z*-statistic mask ($R^2 = 0.77$; $t = 5.58$; $P < 0.001$) and the (**E**) gray matter mask ($R^2 = 0.81$; $t = 6.53$; $P < 0.001$). For (**E**), when the two signal change points at the positive extreme are removed, $R^2 = 0.74$; $t = 5.33$; $P < 0.001$. These data outline the degree of repeatability for the experimental gas setup. For panels (**D**) and (**E**), green = hypercapnic–normoxia interleaved with room air (*HC-NO/RA*), blue = hypercapnic–hyperoxia interleaved with hyperoxia (*HC-HO/HO*), and red = hypercapnic–hyperoxia interleaved with room air (*HC-HO/RA*); dashed line is a line of unity.

HO/RA fractional signal change map. The four signal change maps were scaled to the same intensity to demonstrate that *HC-NO/RA*, *HC-HO/HO*, and *HO/RA* yield similar CVR contrasts, while *HC-HO/RA* greatly enhances areas of CVR. Figure 5B demonstrates that scaling the *HC-HO/RA* differently to reflect a contrast similar to the other maps yields a fractional signal change map with similar spatial CVR information. Overall, these maps demonstrate that, although the different hypercapnic pairings exhibit varied signal changes, they convey similar information. Mean signal changes and standard deviations were calculated for the three stimulus pairings of interest, along with *HO/RA*, using both the activation and GM masks, respectively: *HO/RA* = 0.027 ± 0.014 and 0.011 ± 0.007; *HC-NO/RA* = 0.034 ± 0.007 and 0.014 ± 0.004; *HC-HO/HO* = 0.044 ± 0.014 and 0.020 ± 0.008; *HC-HO/RA* = 0.084 ± 0.017 and 0.035 ± 0.010. The GM values are graphically shown in Figure 5C. Bonferroni corrected paired *t*-tests for the contrasts of interest ($P < 0.017$) indicate similar statistical relationships between signal changes when using either activation or GM masks. Bonferroni-corrected paired *t*-test results are as follows (presented as: activation mask; GM mask): *HC-HO/RA* elicited significantly greater signal changes than *HC-HO/HO* ($P < 0.001$; $P < 0.001$) and *HC-NO/RA* ($P < 0.001$; $P < 0.001$); and *HC-HO/HO* elicited significantly higher signal change than *HC-NO/RA* ($P = 0.015$; $P = 0.004$).

Quantitative Changes in Blood Oxygenation and R_2^*

We modeled Y_v during the various gas stimuli by estimating GM signal change values for GM based on measured (Table 1) and known tissue physiology and MR values for *HO/RA*, *HC-NO/RA*, *HC-HO/HO*, and *HC-HO/RA*.

All multivariate fitting was performed using the signal changes in the GM mask to avoid activation criteria from biasing the voxel composition. Under the first estimation scenario where $Y_{v,HC\text{-}HO}$, $Y_{v,HC\text{-}NO}$, and $Y_{v,HO}$ were subject to the constraint in 8, $Y_{v,HO} = 0.659$, $Y_{v,HC\text{-}NO} = 0.665$, and $Y_{v,HC\text{-}HO} = 0.710$, using the experimentally measured baseline $Y_v = 0.632$ ($RSS = 0.075$ and $R^2 = 0.767$). Calculated signal changes were *HO/RA* = 0.0121; *HC-NO/RA* = 0.0137; *HC-HO/HO* = 0.0206; and *HC-HO/RA* = 0.0329. Under the second scenario where Y_v values were not subject to the constraint of 8, $Y_{v,HO} = 0.660$, $Y_{v,HC\text{-}NO} = 0.665$, and $Y_{v,HC\text{-}HO} = 0.712$ ($RSS = 0.065$ and $R^2 = 0.814$). Calculated signal changes were *HO/RA* = 0.0125; *HC-NO/RA* = 0.0137; *HC-HO/HO* = 0.0210; and *HC-HO/RA* = 0.0338. Fitted and experimental results are shown in Figure 5C and results from the fitting procedure, including arterial, venous, and tissue R_2^* values for the gas stimuli, are presented in Table 2.

Figure 5D demonstrates Y_v estimations for the different gas stimuli from the multivariate fitting for several different variations of potentially reasonable physiologic assumptions. The reference fitting, same as the unconstrained fitting shown in Figure 5C, assumes Grubb's $\alpha = 0.38$, no *CBV* change during *HO* (*CBV* = 0.055 mL/mL; $fb_{v,base} = 0.7$), no CBV_v change during *HC-NO* or *HC-HO* (*CBV* = 0.0574 mL/mL; $fb_{v,act} = 0.671$), and no $R_{1,v}$ change during *HO* or *HC-HO*. Overall we find that isolated alterations to any of these parameters (over reasonable ranges) have a small effect on Y_v values, with the potential exception of reducing total *CBV* (condition: *CBV* = 0.047 mL/mL), which noticeably increases Y_v.

DISCUSSION

We examined the effects of interleaving a *HC-HO* vasoactive stimulus with baseline *HO* to understand confounds elicited by *HC-HO* during BOLD-weighted CVR imaging and to quantify changes in blood oxygenation levels that result from different commonly used gas stimuli. The main findings from this study are: (i) administration of baseline HO before a *HC-HO* stimulus significantly reduces the BOLD signal change relative to *HC-HO* interleaved with *RA* and results in BOLD signal changes that are similar to, but significantly greater than, simple *HC-NO* stimuli; (ii)$Y_{v,HC-HO}$ depends on only a small interaction effect from hyperoxia and hypercapnia and within error this parameter is approximately the additive effect of separate hypercapnic and hyperoxic changes; (iii) using previously published blood and tissue R_2^* models, GM parenchymal venous oxygenation (Y_v) is on average approximately 0.712 for *HC-HO*, suggesting that even when excess O_2 is heavily loaded into arterial blood plasma using a 95% O_2 respiratory stimulus, the excess O_2 dissolved in blood plasma leads to only a moderate increase in Y_v relative to hypercapnic normoxic administration ($Y_{v,HC-NO}$≈0.665 and $Y_{v,HC-HO}$≈0.712), using a measured baseline Y_v = 0.632, and (iv) changes in parameter assumptions over a physiologic range, such as whether CBV_v changes during hypercapnia, $R_{1,v}$ changes with hyperoxia, a different Grubb exponent is used, or hyperoxia has a small effect on vasoconstriction, have minimal effects on the estimated Y_v.

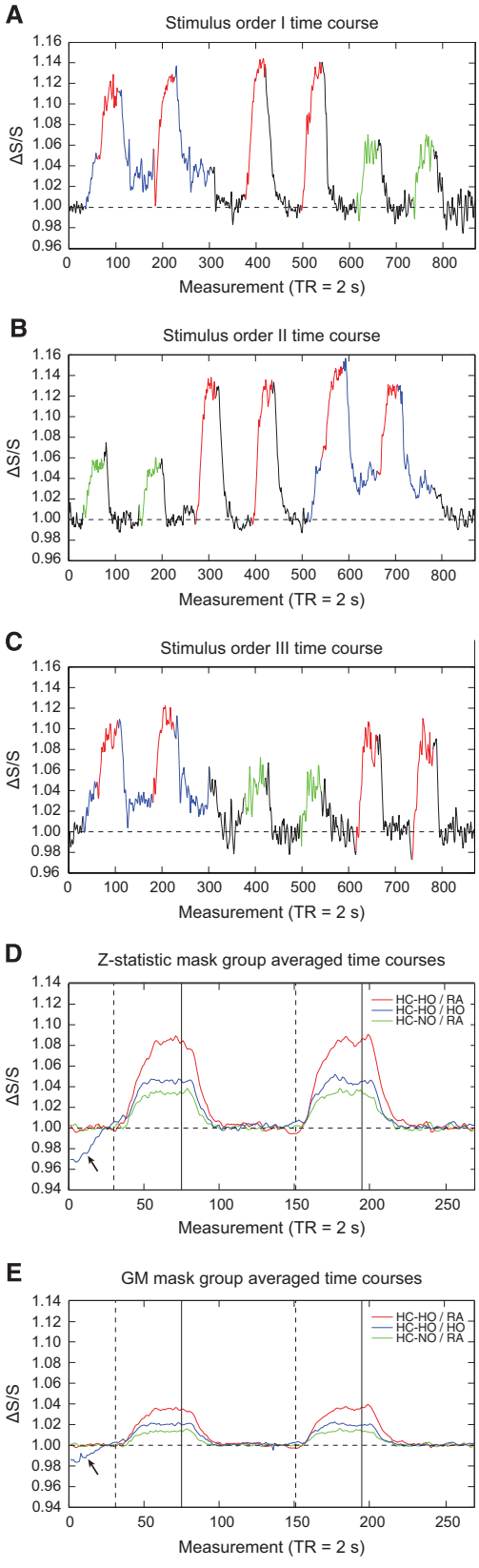

Figure 3. Stimulus ordering and group averaged time courses. (**A**–**C**) Time courses from representative subjects with different gas orderings demonstrate the elicited signal changes. Signal changes were extracted using the *Z*-statistic mask. Black = room air (*RA*), blue = hyperoxia (*HO*), green = hypercapnic–normoxia (*HC-NO*), and red = hypercapnic–hyperoxia (*HC-HO*). (**D** and **E**) Group-averaged time courses calculated using the (**D**) *Z*-statistic activation mask and (**E**) gray matter mask. These time courses demonstrate that similar relative trends are apparent whether evaluating voxels that fall within the *Z*-statistic activation mask ($Z \geqslant 2$) or the gray matter mask. Signal change magnitudes for the latter are reduced, however. Dashed lines indicate start of the respiratory stimulus, while solid lines indicate end of the respiratory stimulus. Black arrows indicate rise in initial hyperoxia (*HO*) baseline signal before the signal plateau.

BOLD Physiology in the Context of Hypercapnic Hyperoxia

The BOLD effect arises owing to fractional decreases in paramagnetic deoxy-hemoglobin (dHb) relative to diamagnetic oxy-hemoglobin (HbO_2), primarily in capillary and venous blood water, which manifests as a shortening of both the intravascular blood and tissue water R_2 and R_2^*. At 3 T, cerebral BOLD effects are approximately 70% extravascular and 30% intravascular[41,42] and depend sensitively on the amount of blood oxygenation. Such blood oxygenation changes are generally a result of the large fractional change in *CBF* relative to *CBV* and $CMRO_2$ but can also be altered by increasing dissolved O_2 in plasma via *HO* gas administration. Although dissolved O_2 does not contribute directly to BOLD contrast, at least three potential and interrelated effects of *HO* will elevate the BOLD contrast in and around the draining vasculature, which are of concern to studies seeking to accurately assess cerebrovascular functioning and reserve. First, O_2 dissolved in plasma from a 95% O_2/5% N_2 respiratory stimulus will significantly elevate PaO_2 (~400 to 600 mm Hg increase),[23,43–46] potentially leading to significant increases in venous HbO_2 saturation which would not occur under normoxic physiologic conditions (PaO_2 = 75 to 100 mm Hg; PvO_2 = 30 to 40 mm Hg). The results of this study indicate that in GM masks the venous blood oxygenation saturation levels (Table 2) are only marginally higher than for *HC-NO* stimuli, suggesting that even when the fraction of inspired O_2 is 95%, there is insufficient O_2 dissolved in venous blood plasma for HbO_2 to increase to near arterial levels. This is consistent with previous data demonstrating that under hyperoxic

conditions jugular PvO_2 increases by 3 to 6 mm Hg, with hyperoxia administration of either 100% O_2 or $PaO_2 = 400$ mm Hg, respectively.[45,47] A second and more probable mechanism to be considered which may contribute to increased venous HbO_2 during hyperoxia is that the increased PaO_2 may reduce the amount of bound O_2 released from Hb to the tissue. Third, and relatedly, as a small percentage of O_2 delivered to tissue is from O_2 dissolved in plasma (~2% of total blood O_2 content), under 95% O_2 administration approximately 5% of total O_2 will be dissolved in the plasma which may slightly increase O_2 transport from the plasma and yield a higher HbO_2 in veins.

Our fitting results suggest that blood oxygenation levels during *HC-HO* are approximately equal to levels that would be expected from administration of separate *HC* and *HO* administration. However, the BOLD signal change between the two situations is slightly different. This is consistent with what is expected from the Bohr and Haldane effects for these levels of *HC* and *HO*. Under *HC-NO* conditions, the Bohr effect dictates that the O_2 dissociation curve (HbO_2 percentage saturation vs. PO_2) shifts to the right, as a result of increased PCO_2, which decreases the affinity of the heme groups to O_2 and facilitates easier unloading of oxygen. During *HO*–normocarbic conditions, the Haldane effect dictates that the CO_2 dissociation curve ($HbCO_2$ percentage saturation vs. PCO_2) shifts because of increased PO_2. This results in decreased heme affinity for CO_2 and facilitates unloading of CO_2. Please refer to Supplementary Figure S1 for a graphical depiction of the Bohr and Haldane effects on blood CO_2 and O_2 content, as well as HbO_2 saturation. The simulations presented in Supplementary Figure S1 suggest that the shift in Hb saturation curves is small over the range of PO_2 and PCO_2 levels considered in this study. Although it is possible that these effects could contribute to the higher *HC-HO*/*HO* signal change relative to *HC-NO*/*RA*, it is also possible that *HO* has a small vasoconstrictive effect, which would lower *CBF* and the BOLD baseline signal, leading to a different fractional signal change. Additionally, similar BOLD effects have been observed in task-evoked BOLD with and without *HO*.[48] For substantially increased venous blood oxygenation that occurs during hypercapnic hyperoxic stimuli, any small increase in venous *CBV* would result in a smaller reduction in the BOLD signal relative to the same *CBV* change that occurs in response to a hypercapnic normoxic stimulus. This is simply due to the lower dHb fraction in the blood in the hypercapnic hyperoxic stimulus. Enhanced BOLD signal changes during *HC-HO* could also potentially result from changes in respiration between hyperoxia and normoxia breathing. In a previous study, it was shown that ventilation did not differ between *HC-HO* and *HC-NO*[24] for short stimulus durations; however, it is logical that ventilation could change slightly between normocapnic hyperoxia and normoxia. An additional possibility related to a larger reduction in oxygen extraction fraction with *HC-HO* relative to *HC-NO* is also possible; however, these effects require further investigation.

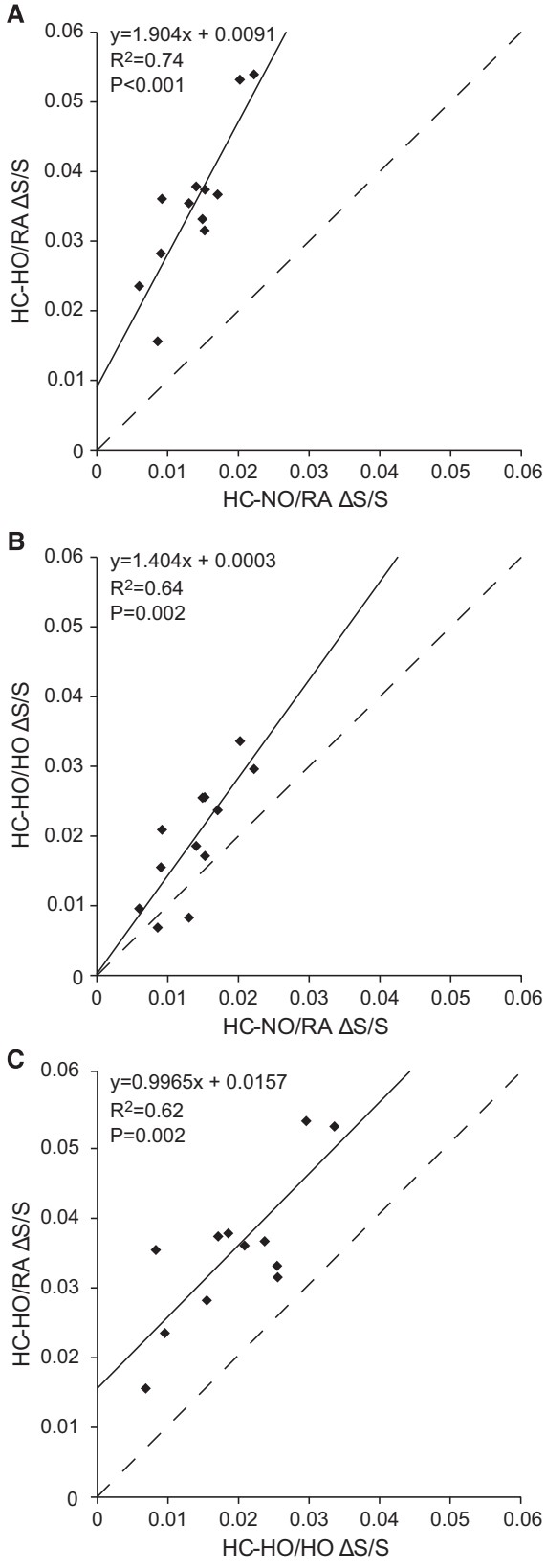

Figure 4. Comparison of blood-oxygenation-level-dependent signal changes (*ΔS/S*) for different respiratory challenges. (**A**) As expected, the fractional signal change elicited from pairing hypercarbic–hyperoxia (*HC-HO*) with a baseline period of room air (*RA*) is greater than that elicited from pairing hypercarbic–normoxia (*HC-NO*) with a baseline period of *RA*. Note that the slope is >1 and intercept is >0. Across subjects, these stimuli exhibit a strong correlation ($R^2 = 0.74$). (**B**) *HC-HO*/*HO* pairing yields a more comparable fractional signal change to *HC-NO*/*RA*, with intercept of 0 and slope closer, but not equal, to unity. This gas pairing also demonstrates a strong correlation with *HC-NO*/*RA* ($R^2 = 0.64$). (**C**) Comparison between *HC-HO*/*HO* and *HC-HO*/*RA* demonstrates that the fractional signal change elicited by *HC-HO*/*RA* is greater than *HC-HO*/*HO*; a strong correlation ($R^2 = 0.62$) is also observed between these stimuli and the slope is near unity. No data points were found to be outliers (>2 standard deviations from the group mean). Dashed line indicates line of unity.

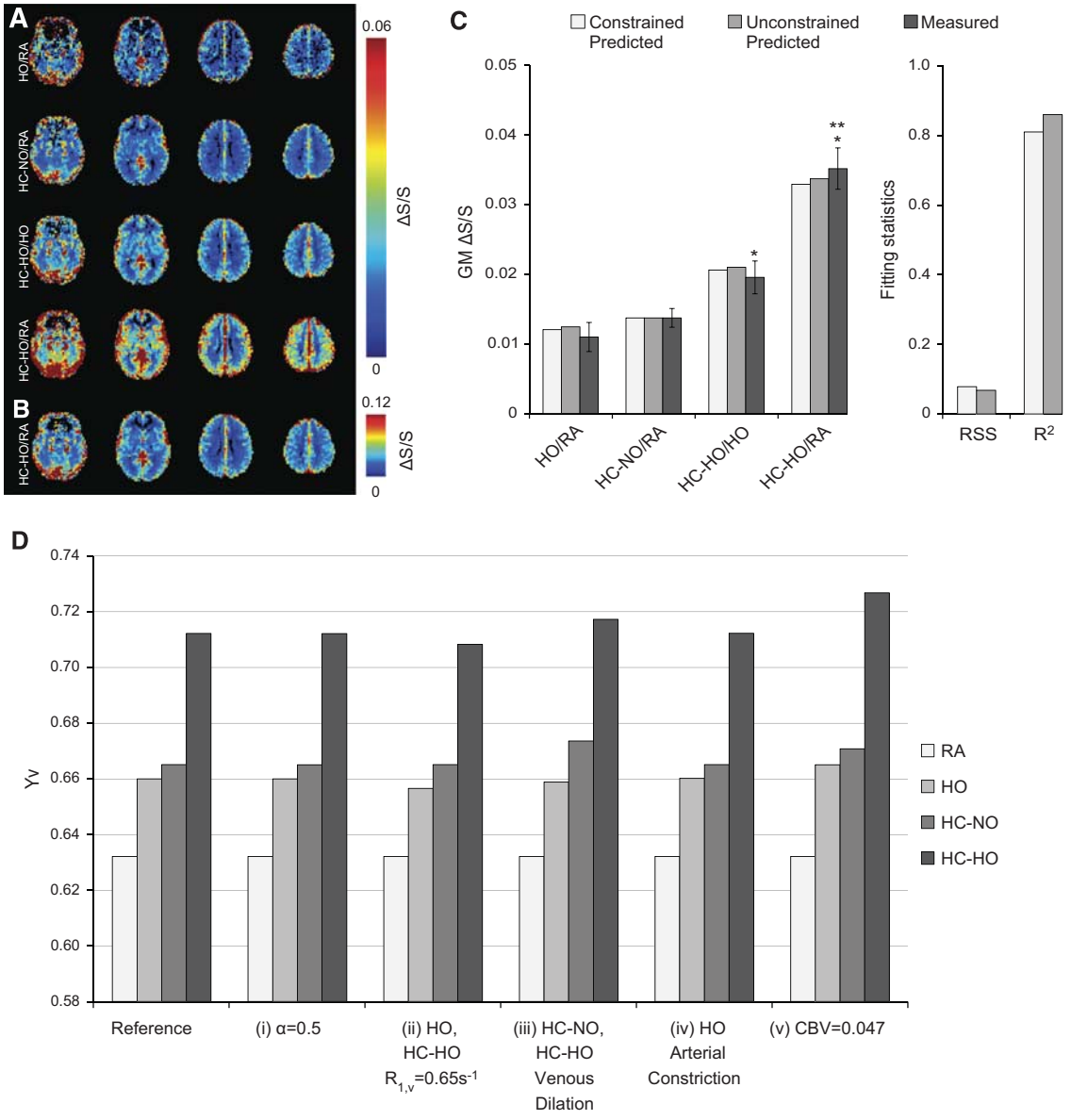

Figure 5. Group averaged fractional signal change maps, multivariate signal change fitting, and simulated effects of changes to physiologic assumptions on Y_v. (**A**) Fractional signal change maps for the gas pairings demonstrate hypercapnic–hyperoxia (*HC-HO*) interleaved with room air (*HC-HO/RA*) exhibits significantly elevated signal change compared with other gas stimuli. (**B**) Hypercapnic–hyperoxia interleaved with room air (*HC-HO/RA*) scaled to similar contrast as other gas pairings. (**C**) Measured and predicted gray matter signal change bar graphs for the three gas pairings of interest plus hyperoxia (*HO*) interleaved with room air (*HO/RA*). Error bars for the measured gray matter signal represent the standard error. For the measured values, *significantly $>$*HC-NO/RA*; **significantly $>$*HC-HO/HO*. Measured signal changes were significantly different across all stimulus pairings of interest; this excludes *HO/RA* for which *t*-tests were not calculated owing to only one stimulus block of this condition being applied (see Methods). (**D**) Simulated effects of changes to physiologic assumptions on Y_v. Here we have systematically changed our physiologic assumptions to demonstrate the potential impact these assumptions have on Y_v for the three gas stimuli: hyperoxia (*HO*), hypercapnic–normoxia (*HC-NO*), and hypercapnic–hyperoxia (*HC-HO*). Specifically, (i) we changed Grubb's α, which dictates the relationship between cerebral blood volume (*CBV*) and cerebral blood flow, from 0.38 to 0.5, (ii) we allowed for hyperoxic gases (*HO* and *HC-HO*) to also reduce $R_{1,v}$, (iii) we allowed for both hypercapnic gases (*HC-NO* and *HC-HO*) to elicit venous vasodilation instead of only arterial dilation, (iv) we allowed for *HO* to elicit arterial vasoconstriction (0.001 mL/mL), and (v) we changed our assumption of the baseline gray matter *CBV* from 0.055 mL/mL to 0.047 mL/mL.

Finally, to further understand how alterations of physiologic or MRI parameters affect fractional signal change and therefore the Y_v level necessary to maintain those changes, we altered several of the assumptions made in our unconstrained, reference simulation (Figure 5D). These alterations included: (i) increasing the Grubb coefficient from $\alpha = 0.38$ to 0.50, (ii) assuming arterial and venous R_1 increases for *HO* and *HC-HO* stimuli, such that *HO* $R_{1,v} = 0.65$/s, (iii) assuming venous dilation occurs during *HC-NO* and *HC-HO*, such that fractional arterial and venous contributions are always maintained at $fb_{a,act} = 0.3$ and $fb_{v,act} = 0.7$, (iv) assuming *HO* causes mild arterial vasoconstriction, such that total *CBV* = 0.054 mL/mL and the respective blood compartment contributions are

$fb_{a,act} = 0.287$ and $fb_{v,act} = 0.713$, and (v) assuming total baseline $CBV = 0.047$ mL/mL instead of $CBV = 0.055$ mL/mL. Our simulations demonstrate that these alterations do relatively little to alter the relationships between the calculated Y_v for the gas stimuli used in this study, with the exception of (v), which increases Y_v for *HO*, *HC-NO*, and *HC-HO* respectively.

Our results suggest that *HC-HO* gas stimuli interleaved with a *HO* baseline provide slightly higher BOLD responses relative to *HC-NO* stimuli interleaved with a normoxic baseline (Figure 5C). We did find significant correlations for BOLD signal changes between all stimulus types (Figure 4). At first this may seem contradictory to a recent study by Hare *et al*.[21] which concluded that there was no correlation between the *HC-HO* and *HC-NO* BOLD responses. However, the sample size in the study of Hare *et al*.[21] was smaller ($n = 8$) and the correlation value reported resulted in a significance level of $P = 0.07$, and therefore it is possible that the study was moderately underpowered to test this specific comparison. Additional differences could be related to the shorter baseline period allowed for the signal to normalize between respiratory challenges and baseline modeling that was performed and/or a lack of sufficient range to evaluate correlations (e.g., two data points were classified as outliers and removed).

It should be noted that it is critical to incorporate extravascular R_2^* effects into quantification models, as was done here. This is simply due to the tissue occupying such a large fraction of the GM parenchymal voxels (approximately 95%) even though HbO_2/dHb changes occur in blood. If only intravascular models are included, it is found that Y_v is much higher (near 100%) for *HC-HO* administration; however, this assumption is incorrect.

Limitations

First, *Z*-statistic activation masks were used to present a portion of the signal change results and time courses. These masks represented all voxels that exhibited statistically significant positive signal increases ($Z \geqslant 2$) across all gas pairings of interest. This approach was used to ensure that voxels responding to all gas stimuli were evaluated. This approach, however, had two effects; (i) values were extracted from overall parenchyma but are inherently biased toward voxels with high venous *CBV* fractions (as is the case with most BOLD fMRI activation maps) and (ii) signal changes are inherently larger than those reported for segmented GM masks that do not bias the activation map in favor of high venous *CBV* fractions. For these reasons, we used the GM masks for all multivariate fitting, as the voxel composition in these masks is expected to be more representative of tissue and volume fractions in the physiology literature. Accordingly, results from this study should not be directly applied to activation maps that may contain larger fractions of draining venous blood.

Second, we did not use a multi-echo acquisition to calculate R_2^* values during administration of the various gas stimuli but rather performed multivariate fitting using established models to calculate R_2^* and Y_v based on calculated GM signal changes. However, such multi-echo experiments would be useful in the future (at the cost of temporal resolution), as the majority of such experiments have only been performed for neuronal, rather than vascular, stimuli.[41,42] Relatedly, it may have been beneficial to use TRUST MRI[25,26] during administration of all gas stimuli. In separate work we pursued this; however, it is unclear whether TRUST MRI performed during hyperoxia provides an accurate measure of microvascular blood oxygenation, as the venous blood water R_2 measure is made in the superior sagittal sinus, at which point Y_v values may differ relative to upstream GM.

Third, our multivariate fitting results for Y_v demonstrated that the unconstrained fitting yielded a better fit and minimized the error relative to the constrained fitting. This is not surprising as a constrained fitting routine will always yield a poorer fit relative to an unconstrained fit. Data from both fitting procedures, however, indicate that relatively minimal fractional differences in Y_v are found with vs. without the specified constraint.

Fourth, our physiologic results indicate that $EtCO_2$ values reduced on average by 1.17 mm Hg during *HO* administration. This is consistent with a recently published study indicating 1.1 and 0.6 mm Hg average reductions in $EtCO_2$ during 3-minute long blocks of 50% *HO* administration under two separate runs, respectively.[49] However, this value is also somewhat smaller than what has been reported in other studies.[23,44]

Finally, we did not monitor EtO_2 levels, as it was assumed that EtO_2 was similar for all healthy volunteers for the same stimuli.

CONCLUSION

We have demonstrated that more comparable BOLD signal changes to standard *HC-NO* paired with baseline *RA* can be achieved by using *HC-HO* with baseline *HO*, rather than baseline *RA*. However, this still yields significantly higher fractional signal changes than when pairing *HC-NO* with a baseline period of *RA*. Y_v resulting from *HC-HO* administration is similar, but not identical, to the summation of separate contributions from *HO* and *HC*. These differences should be considered when comparing BOLD or *CBF* responses measured from respiratory challenges with hyperoxic components. For pure CVR assessment, it is simplest and advisable to use a basic *HC-NO* stimulus when feasible; however, *HC-HO* may be useful with a *HO* baseline to assess CVR when examining potentially hypoxic patients for whom *HC-NO* stimuli may be contraindicated.

AUTHOR CONTRIBUTIONS

Carlos C Faraco: Involved in experimental design, model derivation, data acquisition, analysis, interpretation, and manuscript drafting and revision. Megan K Strother and Lori C Jordan: Involved in experimental design, data interpretation, and manuscript revision. Jeroen CW Siero: Involved in data acquisition, model derivation, interpretation, and manuscript revision. Daniel F Arteaga: Involved in data acquisition and manuscript revision. Allison O Scott: Involved in data interpretation and manuscript revision. Manus J Donahue: Involved in experimental design, model derivation, data acquisition, analysis, interpretation, and manuscript revision.

DISCLOSURE/CONFLICT OF INTEREST

The authors declare no conflict of interest.

ACKNOWLEDGMENTS

The authors thank David Pennell, Leslie McIntosh, Kristen George-Durrett, Clair Kurtenbach, Charles Nockowski, and Christopher Thompson for experimental support.

REFERENCES

1 Faraco CC, Strother MK, Dethrage LM, Jordan L, Singer R, Clemmons PF *et al.* Dual echo vessel-encoded ASL for simultaneous BOLD and CBF reactivity assessment in patients with ischemic cerebrovascular disease. *Magn Reson Med* 2015; **73**: 1579–1592.
2 Mandell DM, Han JS, Poublanc J, Crawley AP, Stainsby JA, Fisher JA *et al.* Mapping cerebrovascular reactivity using blood oxygen level-dependent MRI in patients with arterial steno-occlusive disease: comparison with arterial spin labeling MRI. *Stroke* 2008; **39**: 2021–2028.
3 Thomas BP, Yezhuvath US, Tseng BY, Liu P, Levine BD, Zhang R *et al.* Life-long aerobic exercise preserved baseline cerebral blood flow but reduced vascular reactivity to CO_2. *J Magn Reson Imaging* 2013; **38**: 1177–1183.
4 Yezhuvath US, Lewis-Amezcua K, Varghese R, Xiao G, Lu H. On the assessment of cerebrovascular reactivity using hypercapnia BOLD MRI. *NMR Biomed* 2009; **22**: 779–786.
5 Bokkers RP, van Osch MJ, Klijn CJ, Kappelle LJ, Hendrikse J. Cerebrovascular reactivity within perfusion territories in patients with an internal carotid artery occlusion. *J Neurol Neurosurg Psychiatry* 2011; **82**: 1011–1016.

6 Siero JC, Hartkamp NS, Donahue MJ, Harteveld AA, Compter A, Petersen ET *et al.* Neuronal activation induced BOLD and CBF responses upon acetazolamide administration in patients with steno-occlusive artery disease. *Neuroimage* 2015; **105**: 276–285.
7 Bright MG, Donahue MJ, Duyn JH, Jezzard P, Bulte DP. The effect of basal vasodilation on hypercapnic and hypocapnic reactivity measured using magnetic resonance imaging. *J Cereb Blood Flow Metab* 2011; **31**: 426–438.
8 Warnert EA, Harris AD, Murphy K, Saxena N, Tailor N, Jenkins NS *et al.* In vivo assessment of human brainstem cerebrovascular function: a multi-inversion time pulsed arterial spin labelling study. *J Cereb Blood Flow Metab* 2014; **34**: 956–963.
9 Conklin J, Fierstra J, Crawley AP, Han JS, Poublanc J, Silver FL *et al.* Mapping white matter diffusion and cerebrovascular reactivity in carotid occlusive disease. *Neurology* 2011; **77**: 431–438.
10 Donahue MJ, Dethrage LM, Faraco CC, Jordan LC, Clemmons P, Singer R *et al.* Routine clinical evaluation of cerebrovascular reserve capacity using carbogen in patients with intracranial stenosis. *Stroke* 2014; **45**: 2335–2341.
11 Sobczyk O, Battisti-Charbonney A, Poublanc J, Crawley AP, Sam K, Fierstra J *et al.* Assessing cerebrovascular reactivity abnormality by comparison to a reference atlas. *J Cereb Blood Flow Metab* 2015; **35**: 213–220.
12 Arteaga DF, Strother MK, Faraco CC, Jordan LC, Ladner TR, Dethrage LM *et al.* The vascular steal phenomenon is an incomplete contributor to negative cerebrovascular reactivity in patients with symptomatic intracranial stenosis. *J Cereb Blood Flow Metab* 2014; **34**: 1453–1462.
13 Mandell DM, Han JS, Poublanc J, Crawley AP, Fierstra J, Tymianski M *et al.* Quantitative measurement of cerebrovascular reactivity by blood oxygen level-dependent MR imaging in patients with intracranial stenosis: preoperative cerebrovascular reactivity predicts the effect of extracranial-intracranial bypass surgery. *AJNR Am J Neuroradiol* 2011; **32**: 721–727.
14 Conklin J, Fierstra J, Crawley AP, Han JS, Poublanc J, Mandell DM *et al.* Impaired cerebrovascular reactivity with steal phenomenon is associated with increased diffusion in white matter of patients with Moyamoya disease. *Stroke* 2010; **41**: 1610–1616.
15 Fierstra J, Poublanc J, Han JS, Silver F, Tymianski M, Crawley AP *et al.* Steal physiology is spatially associated with cortical thinning. *J Neurol Neurosurg Psychiatry* 2010; **81**: 290–293.
16 Donahue MJ, Ayad M, Moore R, van Osch M, Singer R, Clemmons P *et al.* Relationships between hypercarbic reactivity, cerebral blood flow, and arterial circulation times in patients with moyamoya disease. *J Magn Reson Imaging* 2013; **38**: 1129–1139.
17 Sam K, Small E, Poublanc J, Han JS, Mandell DM, Fisher JA *et al.* Reduced contralateral cerebrovascular reserve in patients with unilateral steno-occlusive disease. *Cerebrovasc Dis* 2014; **38**: 94–100.
18 Ashkanian M, Gjedde A, Mouridsen K, Vafaee M, Hansen KV, Ostergaard L *et al.* Carbogen inhalation increases oxygen transport to hypoperfused brain tissue in patients with occlusive carotid artery disease: increased oxygen transport to hypoperfused brain. *Brain Res* 2009; **1304**: 90–95.
19 Ashkanian M, Borghammer P, Gjedde A, Ostergaard L, Vafaee M. Improvement of brain tissue oxygenation by inhalation of carbogen. *Neuroscience* 2008; **156**: 932–938.
20 Gauthier CJ, Hoge RD. A generalized procedure for calibrated MRI incorporating hyperoxia and hypercapnia. *Hum Brain Mapp* 2013; **34**: 1053–1069.
21 Hare HV, Germuska M, Kelly ME, Bulte DP. Comparison of CO_2 in air versus carbogen for the measurement of cerebrovascular reactivity with magnetic resonance imaging. *J Cereb Blood Flow Metab* 2013; **33**: 1799–1805.
22 Wise RG, Harris AD, Stone AJ, Murphy K. Measurement of OEF and absolute $CMRO_2$: MRI-based methods using interleaved and combined hypercapnia and hyperoxia. *Neuroimage* 2013; **83**: 135–147.
23 Xu F, Liu P, Pascual JM, Xiao G, Lu H. Effect of hypoxia and hyperoxia on cerebral blood flow, blood oxygenation, and oxidative metabolism. *J Cereb Blood Flow Metab* 2012; **32**: 1909–1918.
24 Donahue MJ, Faraco CC, Strother MK, Chappell MA, Rane S, Dethrage LM *et al.* Bolus arrival time and cerebral blood flow responses to hypercarbia. *J Cereb Blood Flow Metab* 2014; **34**: 1243–1252.
25 Lu H, Ge Y. Quantitative evaluation of oxygenation in venous vessels using T_2-Relaxation-Under-Spin-Tagging MRI. *Magn Reson Med* 2008; **60**: 357–363.
26 Lu H, Xu F, Grgac K, Liu P, Qin Q, van Zijl P. Calibration and validation of TRUST MRI for the estimation of cerebral blood oxygenation. *Magn Reson Med* 2012; **67**: 42–49.
27 Xu F, Uh J, Liu P, Lu H. On improving the speed and reliability of T_2-relaxation-under-spin-tagging (TRUST) MRI. *Magn Reson Med* 2012; **68**: 198–204.
28 Smith SM, Jenkinson M, Woolrich MW, Beckmann CF, Behrens TE, Johansen-Berg H *et al.* Advances in functional and structural MR image analysis and implementation as FSL. *Neuroimage* 2004; **23**(Suppl 1): S208–S219.
29 Bianciardi M, Fukunaga M, van Gelderen P, Horovitz SG, de Zwart JA, Duyn JH. Modulation of spontaneous fMRI activity in human visual cortex by behavioral state. *Neuroimage* 2009; **45**: 160–168.
30 Donahue MJ, Hoogduin H, Smith SM, Siero JC, Chappell M, Petridou N *et al.* Spontaneous blood oxygenation level-dependent fMRI signal is modulated by behavioral state and correlates with evoked response in sensorimotor cortex: a 7.0-T fMRI study. *Hum Brain Mapp* 2012; **33**: 511–522.
31 Mazziotta JC, Toga AW, Evans A, Fox P, Lancaster J. A probabilistic atlas of the human brain: theory and rationale for its development. The International Consortium for Brain Mapping (ICBM). *Neuroimage* 1995; **2**: 89–101.
32 Zhao JM, Clingman CS, Narvainen MJ, Kauppinen RA, van Zijl PC. Oxygenation and hematocrit dependence of transverse relaxation rates of blood at 3T. *Magn Reson Med* 2007; **58**: 592–597.
33 Uludag K, Muller-Bierl B, Ugurbil K. An integrative model for neuronal activity-induced signal changes for gradient and spin echo functional imaging. *Neuroimage* 2009; **48**: 150–165.
34 Donahue MJ, Blicher JU, Ostergaard L, Feinberg DA, MacIntosh BJ, Miller KL *et al.* Cerebral blood flow, blood volume, and oxygen metabolism dynamics in human visual and motor cortex as measured by whole-brain multi-modal magnetic resonance imaging. *J Cereb Blood Flow Metab* 2009; **29**: 1856–1866.
35 van Zijl PC, Eleff SM, Ulatowski JA, Oja JM, Ulug AM, Traystman RJ *et al.* Quantitative assessment of blood flow, blood volume and blood oxygenation effects in functional magnetic resonance imaging. *Nat Med* 1998; **4**: 159–167.
36 Grubb RL, Jr, Raichle ME, Eichling JO, Ter-Pogossian MM. The effects of changes in $PaCO_2$ on cerebral blood volume, blood flow, and vascular mean transit time. *Stroke* 1974; **5**: 630–639.
37 Diringer MN, Aiyagari V, Zazulia AR, Videen TO, Powers WJ. Effect of hyperoxia on cerebral metabolic rate for oxygen measured using positron emission tomography in patients with acute severe head injury. *J Neurosurg* 2007; **106**: 526–529.
38 Lu H, Clingman C, Golay X, van Zijl PC. Determining the longitudinal relaxation time (T_1) of blood at 3.0 Tesla. *Magn Reson Med* 2004; **52**: 679–682.
39 Ulatowski JA, Oja JM, Suarez JI, Kauppinen RA, Traystman RJ, van Zijl PC. In vivo determination of absolute cerebral blood volume using hemoglobin as a natural contrast agent: an MRI study using altered arterial carbon dioxide tension. *J Cereb Blood Flow Metab* 1999; **19**: 809–817.
40 Spees WM, Yablonskiy DA, Oswood MC, Ackerman JJ. Water proton MR properties of human blood at 1.5 Tesla: magnetic susceptibility, T(1), T(2), T*(2), and non-Lorentzian signal behavior. *Magn Reson Med* 2001; **45**: 533–542.
41 Donahue MJ, Hoogduin H, van Zijl PC, Jezzard P, Luijten PR, Hendrikse J. Blood oxygenation level-dependent (BOLD) total and extravascular signal changes and $DeltaR_2$* in human visual cortex at 1.5, 3.0 and 7.0 T. *NMR Biomed* 2011; **24**: 25–34.
42 Lu H, van Zijl PC. Experimental measurement of extravascular parenchymal BOLD effects and tissue oxygen extraction fractions using multi-echo VASO fMRI at 1.5 and 3.0 T. *Magn Reson Med* 2005; **53**: 808–816.
43 Haddock B, Larsson HB, Hansen AE, Rostrup E. Measurement of brain oxygenation changes using dynamic T(1)-weighted imaging. *Neuroimage* 2013; **78**: 7–15.
44 Gauthier CJ, Desjardins-Crepeau L, Madjar C, Bherer L, Hoge RD. Absolute quantification of resting oxygen metabolism and metabolic reactivity during functional activation using QUO_2 MRI. *Neuroimage* 2012; **63**: 1353–1363.
45 Forkner IF, Piantadosi CA, Scafetta N, Moon RE. Hyperoxia-induced tissue hypoxia: a danger? *Anesthesiology* 2007; **106**: 1051–1055.
46 Floyd TF, Clark JM, Gelfand R, Detre JA, Ratcliffe S, Guvakov D *et al.* Independent cerebral vasoconstrictive effects of hyperoxia and accompanying arterial hypocapnia at 1 ATA. *J Appl Physiol (1985)* 2003; **95**: 2453–2461.
47 Matta BF, Lam AM, Mayberg TS. The influence of arterial oxygenation on cerebral venous oxygen saturation during hyperventilation. *Can J Anaesth* 1994; **41**: 1041–1046.
48 Driver ID, Hall EL, Wharton SJ, Pritchard SE, Francis ST, Gowland PA. Calibrated BOLD using direct measurement of changes in venous oxygenation. *Neuroimage* 2012; **63**: 1178–1187.
49 Tancredi FB, Lajoie I, Hoge RD. Test-retest reliability of cerebral blood flow and blood oxygenation level-dependent responses to hypercapnia and hyperoxia using dual-echo pseudo-continuous arterial spin labeling and step changes in the fractional composition of inspired gases. *J Magn Reson Imaging* 2015; doi:10.1002/jmri.24878; e-pub ahead of print.

Supplementary Information accompanies the paper on the Journal of Cerebral Blood Flow & Metabolism website (http://www.nature.com/jcbfm)